

# Hybrid potentials versus gluelumps

Antonio Pineda

*Grup de Física Teòrica and IFAE, Universitat Autònoma de Barcelona, E-08193 Bellaterra,  
Barcelona, Spain*

**Abstract.** A potential model description of heavy quarkonium can be rigorously deduced from QCD under some circumstances. The potentials can be unambiguously related with Wilson loops with gluonic insertions, the spectral decomposition of which is a function of the spectrum and matrix elements solution of the static limit of NRQCD. This spectrum is nothing but the static singlet potential and the hybrid potentials (which correspond to the gluonic excitations). We will quantitatively show that the latter unambiguously relate to the gluelumps at short distances using effective field theories.

**Keywords:** Potentials, heavy quarkonium, effective theories

**PACS:** 12.39.Pn, 12.39.Hg, 12.38.Gc

## INTRODUCTION

Potentials appear in a natural way in the description of systems with slow moving particles like in heavy quarkonium. It is now possible [1, 2] to obtain a potential model-like description of the heavy quarkonium dynamics from first principles using effective field theories under some circumstances (for a review see [3]). The study of these potentials (the static [4] and the relativistic [5, 6, 7] corrections) becomes then crucial as they dictate the dynamic of the heavy quarkonium<sup>1</sup>. They can be obtained from the solution (spectrum and matrix elements) of NRQCD in the static limit. The spectrum of NRQCD directly provides the static singlet potential and the hybrid potentials. Therefore it is interesting to study them on their own. In particular, the study of the hybrid potentials may become important in order to discern whether the recently found resonances near threshold can be understood as hybrid states (see [8] for a review on the different possible interpretation of these new states).

In this review we closely follow [9]. We will focus on the short distance limit of the hybrid potentials, specially on the aspects that can be fixed on symmetry arguments only, and we will quantitatively relate them with the physics of gluelumps.

---

<sup>1</sup> One may wonder why bother to compute these potentials in the lattice, as one may try to do a direct computation of the heavy quarkonium properties in the lattice. Leaving aside the technical difficulties of these direct computations, in the best of the worlds they only provide with a very limited information on the properties of the heavy quarkonium: mainly a few masses (for the ground state and low excitations) and, maybe, some inclusive decays. On the other hand, with the potentials it is possible to obtain a detailed information of the shape of the heavy quarkonium, one can then compute the complete spectrum, all the inclusive decays and also opens the possibility to consider differential decay rates, which are far beyond the possibility of present direct lattice simulations.

## STATIC LIMIT OF pNRQCD

The static limit of NRQCD at short distances can be studied with the static version of pNRQCD. In this limit new symmetries arise.

The pNRQCD Lagrangian at leading order in  $1/m$  and in the multipole expansion reads [10, 11],

$$L_{\text{pNRQCD}} = \int d^3\mathbf{r} d^3\mathbf{R} \text{Tr} \left[ \mathbf{S}^\dagger (i\partial_0 - V_s) \mathbf{S} + \mathbf{O}^\dagger (iD_0 - V_o) \mathbf{O} \right] - \int d^3\mathbf{R} \frac{1}{4} F_{\mu\nu}^a F^{\mu\nu a} + O(r). \quad (1)$$

All the gauge fields in Eq. (1) are evaluated in  $\mathbf{R}$  and  $t$ , in particular  $F^{\mu\nu a} \equiv F^{\mu\nu a}(\mathbf{R}, t)$  and  $iD_0\mathbf{O} \equiv i\partial_0\mathbf{O} - g[A_0(\mathbf{R}, t), \mathbf{O}]$ . The singlet and octet potentials  $V_i$ ,  $i = s, o$  are to be regarded as matching coefficients, which depend on the scale  $v_{us}$  separating soft gluons from ultrasoft ones. In the static limit “soft” energies are of  $O(1/r)$  and “ultrasoft” energies are of  $O(\alpha_s/r)$ . Notice that the hard scale,  $m$ , plays no rôle in this limit. The only assumption made so far concerns the size of  $r$ , i.e.  $1/r \gg \Lambda_{\text{QCD}}$ , such that the potentials can be computed in perturbation theory. Also note that throughout this paper we will adopt a Minkowski space-time notation.

The spectrum of the singlet state reads,

$$E_s(r) = 2m_{\text{OS}} + V_s(r) + O(r^2), \quad (2)$$

where  $m_{\text{OS}}$  denotes an on-shell (OS) mass. One would normally apply pNRQCD to quarkonia and in this case  $m_{\text{OS}}$  represents the heavy quark pole mass. For the static hybrids, the spectrum reads

$$E_H(r) = 2m_{\text{OS}} + V_o(r) + \Lambda_H^{\text{OS}} + O(r^2), \quad (3)$$

where

$$\Lambda_H^{\text{OS}} \equiv \lim_{T \rightarrow \infty} i \frac{\partial}{\partial T} \ln \langle H^a(T/2) \phi(T/2, -T/2) H^b(-T/2) \rangle. \quad (4)$$

$$\begin{aligned} \phi(T/2, -T/2) &\equiv \phi(T/2, \mathbf{R}, -T/2, \mathbf{R}) \\ &= \text{P exp} \left\{ -ig \int_{-T/2}^{T/2} dt A_0(\mathbf{R}, t) \right\}, \end{aligned} \quad (5)$$

denotes the Schwinger line in the adjoint representation and  $H$  represents some gluonic field, for examples see Table 1.

Eq. (3) allows us to relate the energies of the static hybrids  $E_H$  to the energies of the gluelumps,

$$\Lambda_H^{\text{OS}} = [E_H(r) - E_s(r)] - [V_o(r) - V_s(r)] + O(r^2). \quad (6)$$

This equation encapsulates one of the central ideas of this paper. The combination  $E_H - E_s$  is renormalon-free in perturbation theory [up to possible  $O(r^2)$  effects], and can be calculated unambiguously non-perturbatively: the ultraviolet (UV) renormalons related to the infrared (IR) renormalons of twice the pole mass cancel each other. However,  $\Lambda_H$  contains an UV renormalon that corresponds to the leading IR renormalon of  $V_o$ .

## Symmetries of hybrid potentials and gluelumps

The spectrum of open QCD string states can be completely classified by the quantum numbers associated with the underlying symmetry group, up to radial excitations. In this case, these are the distance between the endpoints, the gauge group representation under which these endpoints transform (in what follows we consider the fundamental representation), and the symmetry group of cylindrical rotations with reflections  $D_{\infty h}$ . The irreducible representations of the latter group are conventionally labelled by the spin along the axis,  $\Lambda$ , where  $\Sigma, \Pi, \Delta$  refer to  $\Lambda = 0, 1, 2$ , respectively, with a subscript  $\eta = g$  for gerade (even)  $PC = +$  or  $\eta = u$  for ungerade (odd)  $PC = -$  transformation properties. All  $\Lambda \geq 1$  representations are two-dimensional. The one-dimensional  $\Sigma$  representations have, in addition to the  $\eta$  quantum number, a  $\sigma_v$  parity with respect to reflections on a plane that includes the two endpoints. This is reflected in an additional  $\pm$  superscript. The state associated with the static singlet potential transforms according to the representation  $\Sigma_g^+$  while the two lowest lying hybrid potentials are within the  $\Pi_u$  and  $\Sigma_u^-$  representations, respectively.

In contrast, point-like QCD states are characterised by the  $J^{PC}$  of the usual  $O(3) \otimes \mathcal{C}$  rotation group as well as by the gauge group representation of the source. In the pure gauge sector, gauge invariance requires this representation to have vanishing triality, such that the source can be screened to a singlet by the glue. States created by operators in the singlet representation are known as glueballs, octet states as gluelumps. In contrast to gluelump states, where the octet source propagates through the gluonic background, the normalization of glueball states with respect to the vacuum energy is unambiguous.

Since  $D_{\infty h} \subset O(3) \otimes \mathcal{C}$ , in the limit  $r \rightarrow 0$  certain hybrid levels must become degenerate. For instance, in this limit, the  $\Sigma_u^-$  state corresponds to a  $J^{PC} = 1^{+-}$  state with  $J_z = 0$  while the  $\Pi_u$  doublet corresponds to its  $J_z = \pm 1$  partners. The gauge transformation property of the hybrid potential creation operator will also change in this limit,  $\mathbf{3} \otimes \mathbf{3}^* = \mathbf{1} \oplus \mathbf{8}$ , such that hybrids will either approach gluelumps [cf. Eq. (3)] or glueballs, in an appropriate normalization. In the case of glueballs the correct normalization can be obtained by considering the difference  $E_H(r) - E_S(r)$  from which the pole mass cancels. We will discuss the situation with respect to gluelumps in detail below.

In perturbation theory, the ground state potential corresponds to the singlet potential while hybrid potentials will have the perturbative expansion of the octet potential, which have recently been computed to two loops [15].

## Hybrid and gluelump mass splittings

We would like to establish if lattice data on hybrid potentials reproduces the degeneracies expected from the above discussion in the short distance region. In the limit  $r \rightarrow 0$ , any given  $\Lambda \geq 1$  hybrid potential can be subduced from any  $J^{PC}$  state with  $J \geq \Lambda$  and  $PC = +$  for  $\eta = g$  or  $PC = -$  for  $\eta = u$  representations. For instance the  $\Pi_u$  is embedded in  $1^{+-}, 1^{-+}, 2^{+-}, 2^{-+}, \dots$ . The situation is somewhat different for  $\Lambda = 0$  states, which have the additional  $\sigma_v$  parity: the  $\Sigma_g^+$  representation can be obtained from  $0^{++}, 1^{--}, 2^{++}, \dots$ ,  $\Sigma_g^-$  from  $0^{--}, 1^{++}, \dots$ ,  $\Sigma_u^+$  from  $0^{+-}, 1^{-+}, \dots$  and  $\Sigma_u^-$

**TABLE 1.** Expected degeneracies of hybrid potentials at short distance, based on the level ordering of the gluelump spectrum. Note that if the  $3^{+-}$  gluelump turned out to be lighter than the  $2^{+-}$  then the  $\Sigma_u^-, \Pi_u', \Delta_u, \Phi_u$  potentials would approach the  $3^{+-}$  state while the  $\Sigma_u^+, \Pi_u'', \Delta_u'$  potentials would approach the  $2^{+-}$  instead.

point particle $J^{PC}$	$H$	$\Lambda_H^{\text{RS}} r_0$	$\Lambda_H^{\text{RS}}/\text{GeV}$	open string $\Lambda_\eta^{\sigma_v}$
$1^{+-}$	$B_i$	2.25(39)	0.87(15)	$\Sigma_u^-, \Pi_u$
$1^{--}$	$E_i$	3.18(41)	1.25(16)	$\Sigma_g^+, \Pi_g$
$2^{--}$	$D_{\{i}B_{j\}}$	3.69(42)	1.45(17)	$\Sigma_g^-, \Pi_g', \Delta_g$
$2^{+-}$	$D_{\{i}E_{j\}}$	4.72(48)	1.86(19)	$\Sigma_u^+, \Pi_u', \Delta_u$
$3^{+-}$	$D_{\{i}D_jB_{k\}}$	4.72(45)	1.86(18)	$\Sigma_u^-, \Pi_u'', \Delta_u', \Phi_u$
$0^{++}$	$\mathbf{B}^2$	5.02(46)	1.98(18)	$\Sigma_g^{+''}$
$4^{--}$	$D_{\{i}D_jD_kB_{l\}}$	5.41(46)	2.13(18)	$\Sigma_g^-, \Pi_g'', \Delta_g', \Phi_g, \Gamma_g$
$1^{-+}$	$(\mathbf{B} \wedge \mathbf{E})_i$	5.45(51)	2.15(20)	$\Sigma_u^+, \Pi_u'''$

from  $0^{++}, 1^{+-}, \dots$ . We list all combinations of interest to us in Table 1. The ordering of low lying gluelumps has been established in Ref. [12] and reads with increasing mass:  $1^{+-}, 1^{--}, 2^{--}, 2^{+-}, 3^{+-}, 0^{++}, 4^{--}, 1^{-+}$ , with a  $3^{--}$  state in the region of the  $4^{--}$  and  $1^{-+}$ . The  $2^{+-}$  and  $3^{+-}$  as well as the  $4^{--}$  and  $1^{-+}$  states are degenerate within present statistical uncertainties<sup>2</sup>. The continuum limit gluelump masses are displayed as circles at the left of Fig. 1, where we have added the (arbitrary) overall constant  $2.26/r_0$  to the gluelump splittings to match the hybrid potentials.

Juge, Kuti and Morningstar [13, 14] have comprehensively determined the spectrum of hybrid potentials. We convert their data, computed at their smallest lattice spacing  $a_\sigma \approx 0.2$  fm, into units of  $r_0 \approx 0.5$  fm. Since the results have been obtained with an improved action and on anisotropic lattices with  $a_\tau \approx a_\sigma/4$ , one might expect lattice artifacts to be small, at least for the lower lying potentials. Hence we compare these data, normalized to  $E_{\Sigma_g^+}(r_0)$ , with the continuum expectations of the gluelumps [12]. The full lines are cubic splines to guide the eye while the dashed lines indicate the gluelumps towards which we would expect the respective potentials to converge.

The first 7 hybrid potentials are compatible with the degeneracies suggested by Table 1. The next state is trickier since it is not clear whether  $2^{+-}$  or  $3^{+-}$  is lighter. In the figure we depict the case for a light  $2^{+-}$ . This would mean that  $(\Sigma_u^+, \Pi_u', \Delta_u)$  approach the  $2^{+-}$  while  $(\Sigma_u^-, \Pi_u'', \Delta_u', \Phi_u)$  approach the  $3^{+-}$ . Note that of the latter four potentials only data for  $\Pi_u''$  and  $\Phi_u$  are available. Also note that the continuum states  $\Pi_u', \Pi_u''$  and  $\Phi_u$  are all obtained from the same  $E_u$  lattice representation. For the purpose of the figure we make an arbitrary choice to distribute the former three states among the  $E_u', E_u''$  and  $E_u'''$  lattice potentials. To firmly establish their ordering one would have to investigate radial excitations in additional lattice hybrid channels and/or clarify the gluelump spectrum in more detail. Should the  $2^{+-}$  and  $3^{+-}$  hybrid levels be inverted then  $(\Sigma_u^-, \Pi_u', \Delta_u, \Phi_u)$  will converge to the  $3^{+-}$  while  $(\Sigma_u^+, \Pi_u'', \Delta_u')$  will approach the  $2^{+-}$ . We note that the

<sup>2</sup> The splittings between all states with respect to the  $1^{+-}$  ground state have been extrapolated to the continuum limit in Ref. [12] and we add our own extrapolations for the  $4^{--}$  and  $1^{-+}$  states to these, based on the tables of this reference.

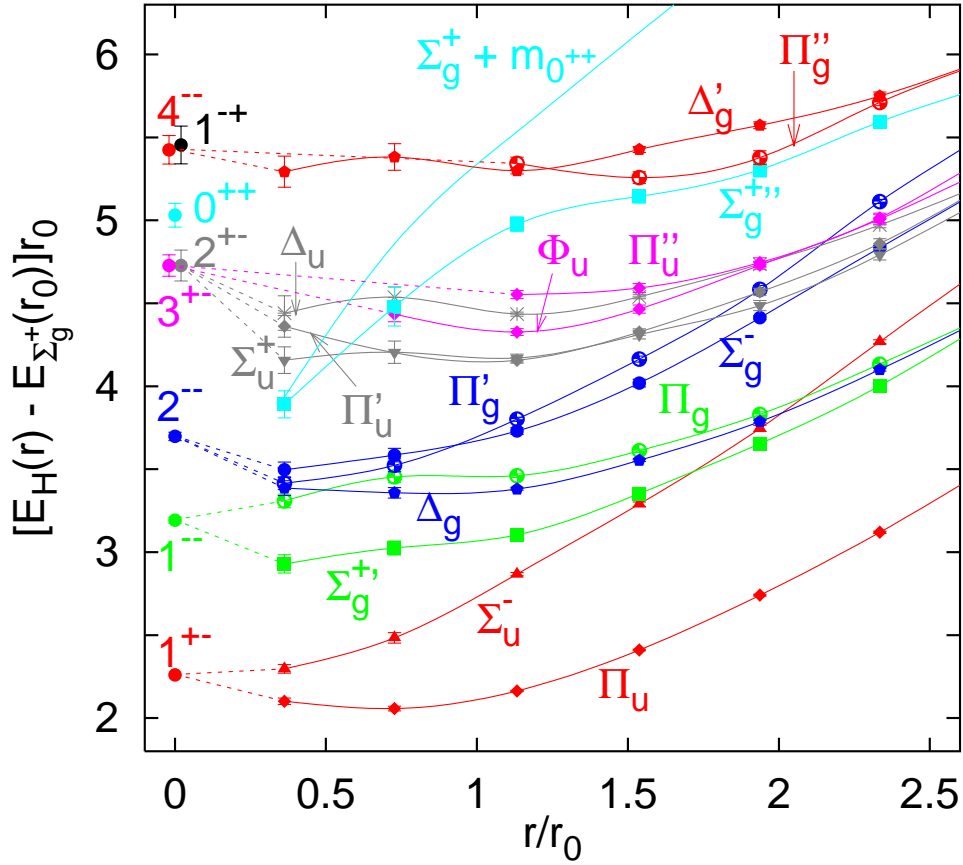


**FIGURE 1.** Different hybrid potentials [14] at a lattice spacing  $a_\sigma \approx 0.2 \text{ fm} \approx 0.4 r_0$ , where  $r_0 \approx 0.5 \text{ fm}$ , in comparison with the gluelump spectrum, extrapolated to the continuum limit [12] (circles, left-most data points). The gluelump spectrum has been shifted by an arbitrary constant to adjust the  $1^{+-}$  state with the  $\Pi_u$  and  $\Sigma_u^-$  potentials at short distance. In addition, we include the sum of the ground state ( $\Sigma_g^+$ ) potential and the scalar glueball mass  $m_{0^{++}}$ . The lines are drawn to guide the eye.

ordering of the hybrid potentials, with a low  $\Sigma_u^+$ , makes the first interpretation more suggestive.

Finally the  $\Sigma_g^{+'}$  potential seems to head towards the  $0^{++}$  gluelump but suddenly turns downward, approaching the (lighter) sum of ground state potential and scalar glueball instead. The latter type of decay will eventually happen for all lattice potentials but only at extremely short distances. We also remark that all potentials will diverge as  $r \rightarrow 0$ . This does not affect our comparison with the gluelump results, since we have normalized them to the  $\Pi_u/\Sigma_u^-$  potentials at the shortest distance available. (The gluelump values are plotted at  $r = 0$  to simplify the figure.)

On a qualitative level the short-distance data are very consistent with the expected degeneracies. From the figure we see that at  $r \approx 2r_0 \approx 1 \text{ fm}$  the spectrum of hybrid potentials displays the equi-distant band structure one would qualitatively expect from a string picture. Clearly this region, as well as the cross-over region to the short-distance behaviour  $r_0 < r < 2r_0$ , cannot be expected to be within the perturbative domain: at best one can possibly imagine perturbation theory to be valid for the left-most 2 data points.

With the exception of the  $\Pi_u$ ,  $\Pi'_u$  and  $\Phi_u$  potentials there are also no clear signs for the onset of the short distance  $1/r$  behaviour with a positive coefficient as expected from perturbation theory. Furthermore, most of the gaps within multiplets of hybrid potentials, that are to leading order indicative of the size of the non-perturbative  $r^2$  term, are still quite significant, even at  $r = 0.4 r_0$ ; for instance the difference between the  $\Sigma_u^-$  and  $\Pi_u$  potentials at this smallest distance is about  $0.28 r_0^{-1} \approx 110$  MeV.

## The difference between the $\Pi_u$ and $\Sigma_u^-$ hybrids

From the above considerations it is clear that for a more quantitative study we need lattice data at shorter distances, which have been obtained for the lowest two gluonic excitations,  $\Pi_u$  and  $\Sigma_u^-$  in Ref. [9]. We display their differences in the continuum limit in Fig. 2. We see how these approach zero at small  $r$ , as expected from the short distance expansion. pNRQCD predicts that the next effects should be of  $O(r^2)$  (and renormalon-free). In fact, we can fit the lattice data rather well with a  $E_{\Pi_u} - E_{\Sigma_u^-} = A_{\Pi_u - \Sigma_u^-} r^2$  ansatz for short distances, with slope (see Fig. 2),

$$A_{\Pi_u - \Sigma_u^-} = 0.92_{-0.52}^{+0.53} r_0^{-3}, \quad (7)$$

where the error is purely statistical (lattice). This fit has been done using points  $r \lesssim 0.5 r_0$ . By increasing the fit range to  $r \lesssim 0.8 r_0$  the following result is obtained,

$$A_{\Pi_u - \Sigma_u^-} = (0.83 \pm 0.29) r_0^{-3}, \quad (8)$$

indicating stability of the result Eq. (7) above.

In order to estimate systematic errors one can add a quartic term:  $br^4$  (only even powers of  $r$  appear in the multipole expansion of this quantity). If the result is stable, our determination of  $A_{\Pi_u - \Sigma_u^-}$  should not change much. Actually this is what happens. If we fit up to  $r \lesssim 0.5 r_0$ , we obtain the central value  $A_{\Pi_u - \Sigma_u^-} r_0^3 = 0.93$  with a very small quartic coefficient,  $br_0^5 = -0.05$ . If we increase the range to  $r \lesssim 0.8 r_0$ , we obtain the same central value,  $A_{\Pi_u - \Sigma_u^-} r_0^3 = 0.93$ , but with a slightly bigger quartic term,  $br_0^5 = -0.18$ . Introducing the quartic term enhances the stability of  $A_{\Pi_u - \Sigma_u^-}$  under variations of the fit range. From this discussion we conclude that the systematic error is negligible, in comparison to the error displayed in our result Eq. (7).

We remark that within the framework of static pNRQCD and to second order in the multipole expansion, one can relate the slope  $A_{\Pi_u - \Sigma_u^-}$  to gluonic correlators of QCD.

## CONCLUSIONS

In conclusion, we have shown that the short distance behavior of the hybrid potentials is consistent with perturbation theory, the operator product expansion (effective field theories), and with the description of the leading non-perturbative effects in this regime in terms of the gluelump masses. For more details see [9].

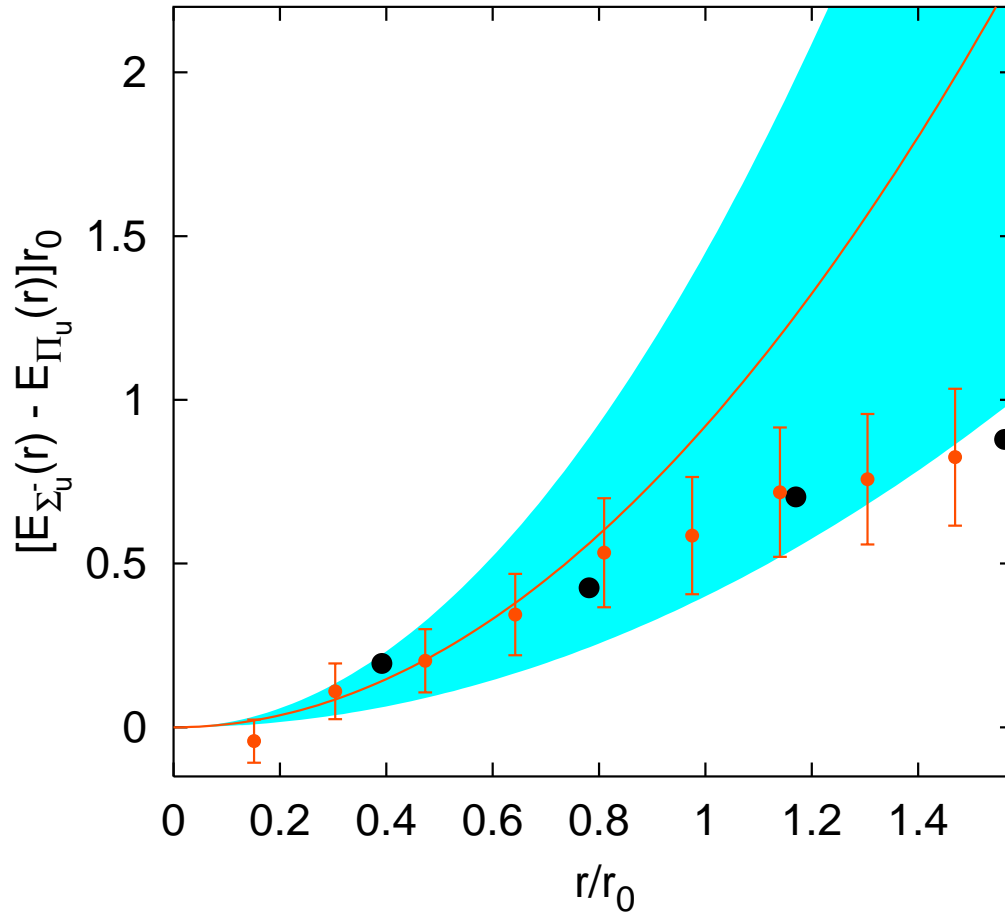


**FIGURE 2.** Splitting between the  $\Sigma_u^-$  and the  $\Pi_u$  potentials, extrapolated to the continuum limit, and the comparison with a quadratic fit to the  $r \lesssim 0.5 r_0$  data points ( $r_0^{-1} \approx 0.4$  GeV). The big circles correspond to the data of Juge et al. [14], obtained at finite lattice spacing  $a_\sigma \approx 0.39 r_0$ . The errors in this case are smaller than the symbols.

## REFERENCES

1. N. Brambilla, A. Pineda, J. Soto and A. Vairo, Phys. Rev. D **63**, 014023 (2001).
2. A. Pineda and A. Vairo, Phys. Rev. D **63**, 054007 (2001) [Erratum-ibid. D **64**, 039902 (2001)].
3. N. Brambilla, A. Pineda, J. Soto and A. Vairo, Rev. Mod. Phys. **77**, 1423 (2005).
4. S. Necco and R. Sommer, Nucl. Phys. B **622**, 328 (2002).
5. G. S. Bali, K. Schilling and A. Wachter, Phys. Rev. D **56**, 2566 (1997).
6. Y. Koma, M. Koma and H. Wittig, arXiv:hep-lat/0607009.
7. Y. Koma and M. Koma, arXiv:hep-lat/0609078.
8. E. Eichten, these proceedings.
9. G. S. Bali and A. Pineda, Phys. Rev. D **69**, 094001 (2004).
10. A. Pineda and J. Soto, Nucl. Phys. Proc. Suppl. **64**, 428 (1998).
11. N. Brambilla, A. Pineda, J. Soto and A. Vairo, Nucl. Phys. B **566**, 275 (2000).
12. M. Foster and C. Michael [UKQCD Collaboration], Phys. Rev. D **59**, 094509 (1999).
13. K. J. Juge, J. Kuti and C. J. Morningstar, Nucl. Phys. Proc. Suppl. **63**, 326 (1998).
14. K. J. Juge, J. Kuti and C. Morningstar, Phys. Rev. Lett. **90**, 161601 (2003).
15. B.A. Kniehl, A.A. Penin, Y. Schroder, V.A. Smirnov and M. Steinhauser, Phys. Lett. B **607**, 96 (2005).